ACS Chemical Neuroscience

Research Article

pubs.acs.org/chemneuro

RNA Based Antagonist of NMDA Receptors

Garam Lee,[†,∥] David M. MacLean,[†,∥] Henning Ulrich,[‡] Xiurong Zhao,[§] Jaroslaw Aronowski,[§] and Vasanthi Jayaraman*[,†]

[†]Center for Membrane Biology, Department of Biochemistry and Molecular Biology, and [§]Department of Neurology, University of Texas Health Science Center, 6431 Fannin, Houston, Texas 77030, United States

[‡]Department of Biochemistry, Instituto de Química, Universidade de São Paulo, São Paulo, Av. Prof. Lineu Prestes 748, São Paulo, S.P. 05508-900, Brazil

ABSTRACT: The *N*-methyl D-aspartate (NMDA) class of ionotropic glutamate receptors plays important roles in learning and memory as well as in a number of neurological disorders including Huntington's disease and cerebral ischemia. Here, we describe the isolation and characterization of a 2′ F-modified RNA aptamers directed against GluN2A-containing NMDA receptors. By adding a negative selection step toward the closely related AMPA and kainate receptors, the RNA aptamers specifically recognize NMDA receptors with dissociation constants in the nanomolar range. Electrophysiological characterization of these aptamers using rapid perfusion in outside-out patches reveals that they selectively inhibit the GluN2A containing subtype of NMDA receptors with little effect on the AMPA and kainate receptor subtypes. We also demonstrate that this RNA aptamer significantly reduces neurotoxicity in an in vitro model of cerebral ischemia. Given that the RNA based antagonist can be readily modified, it can be used as a tool in targeted drug delivery or for imaging purposes in addition to having the potential use as a therapeutic intervention in disorders involving glutamate receptors.

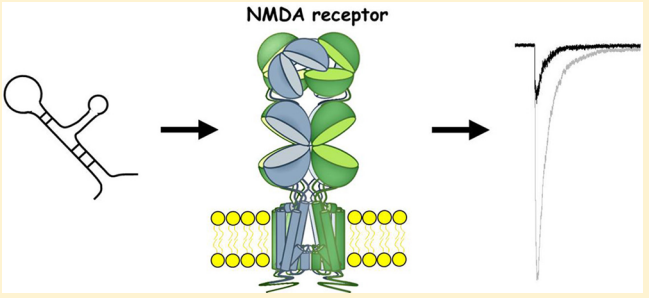

KEYWORDS: *RNA aptamers, NMDA receptors, excitotoxicity, neuroprotection, ligand-gated ion channel, drug discovery*

The *N*-methyl-D-aspartate (NMDA) receptor ion channel is one of the key postsynaptic targets of glutamate mediated synaptic transmission. Synaptic and extrasynaptic NMDA receptors play central roles in physiological processes such as development and synaptic plasticity by allowing glutamate-gated calcium influx into neurons.[1] However, excessive activation of NMDA receptors can lead to excitotoxicity and is associated with several neurological disorders including Parkinson's disease, neuropathic pain and schizophrenia.[2] NMDA receptor antagonists are effective in reducing cerebral infarction in various experimental stroke models[3−6] and have also shown clincal usefulness in the treatment of Alzhiemer's disease[7] and dementia from Parkinson's disease.[8] However, their full theraupeutic potential has not been realized in clinical settings due to severe side effects such as cognitive disruption and pyschotomimetic symptoms.[1,3−6,9] While strong side effects are to some extent more manageable in a transient intervention following ischemia, they present a severe problem in the chronic treatments needed for Alzheimer's disease, Parkinson's disease or schizophrenia. Novel antagonists built from RNA aptamers may offer an alternative to these small molecule drugs.

In general, RNA aptamers have several advantages over traditional small molecule agents. RNA aptamers boast very high affinity and target specificity.[10−13] Indeed in the case of ligand-gated ion channels, aptamers have been evolved which show selectivity for certain functional states over others.[14,15] Moreover, large quantities of aptamers can be chemically synthesized and readily modified to facilitate linkage with lipid or polymer based delivery systems.[10] Such nanoparticle-based delivery systems can alter the biodistribution of these compounds and avoid off-target tissue effects. It is also possible to develop aptamers which specifically pass the blood-brain barrier or show cell specific binding,[10,12,16,17] suggesting the possibility of selectivity for a specific brain region when the correct targeting antibody or aptamer is used. These features endow RNA aptamers with similar binding properties as antibodies but with the added advantage of being non-immunogenic even when administered in excess of therapeutic doses, thus making aptamers an excellent therapeutic candidate for modulating NMDA receptor receptor-dependent signaling pathways.

To move toward developing a highly potent and selective NMDA antagonist from RNA aptamers, we employed an in vitro selection process termed SELEX (Systematic Evolution of Ligands by EXponential enrichment). In this process, RNA aptamers are selected from a library of random nuclease-resistant RNA sequences by repetitive binding of the RNA pool to target molecules of interest. This pool of RNA molecules is

Received: February 25, 2014
Revised: April 7, 2014
Published: April 7, 2014

   dx.doi.org/10.1021/cn500041k | *ACS Chem. Neurosci.* 2014, 5, 559−567

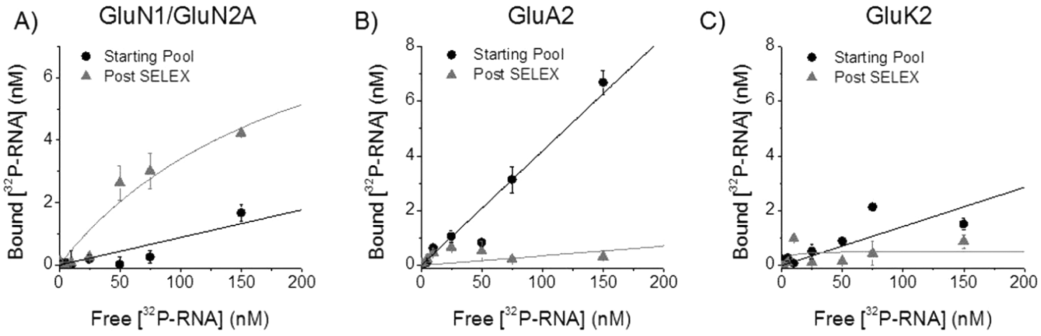

Figure 1. Radioligand binding curves before and after SELEX. (A) Binding curves for the starting pool (black circles) and the pool after 9 rounds of SELEX (gray triangles) on GluN1/GluN2A NMDA receptors. Note saturation binding in the round 9 pool. (B) Similar binding curves on GluA2 AMPA receptors. (C) Binding curves for GluK2 KA receptors.

Table 1. Consensus Motif (bold letters) of Aptamers

aptamer no.	sequences
2	GGG**GCGG**GAGATGGTGTGGTCTCGGGCGGGCGTTAGCGCC
4	AACCTC**GCGGT**CTGTCAGGCTGGCATAGCGAAGGGGCTGG
6	GGCCCCGTGCGTCGCTCCCCGT**GTGGC**TGTGGTTCGTATC
7	TACTGCTTCATACCTGTTGCA**GCGGT**ACCTCCGTAGCGAG
9	TCTTCATTTAATCTTCACCC**CTGGG**CCCTTCCTTTCTCAT
11	AGTTGTCGTG**GTAAGGG**TACTGTAAAGTGAGATTATTGAG
25	GA**GCGCG**CAGTTGGAAAGCTGACAACGCATCTTAAAGCGC
26	GTACGTTCAT**GCGGG**GTCTGTCGTCGGTCGCTGGGAGGC
28	GTCGTGGTTGGCGGAGGGTTTT**GCGGG**TGAAGAGCATGCC
35	AGTACCTGAGCTGGTCGGCGTT**GCGG**GGGTGATACGGTT

subjected to multiple rounds of selective binding to increase the prevalence of high affinity aptamers. To further enhance specificity, we interposed rounds of negative selection against the closely related AMPA and kainate receptors subtypes, selecting out aptamers which show high affinity binding for these subtypes. The resulting candidate aptamers were characterized using radio-ligand binding and electrophysiology. We have isolated an aptamer with a high affinity for the GluN2A containing NMDA receptors (K_d = 120 ± 15 nM) and little to no effect on the closely related GluA2 AMPA receptor and GluK2 kainate receptors. Crucially, this aptamer is neuroprotective in an oxygen glucose deprivation model of ischemia.

RESULTS AND DISCUSSION

As a starting point in developing an NMDA receptor selective RNA antagonist, we used a RNA library containing 10^{15} sequences, each 90 nucleotides long. RNAs were synthesized using 2′-F-pyrimidines instead of 2′-OH-pyrimidines, as these are more resistant to nucleases and show improved stability in the bloodstream.[18] This initial RNA pool was incubated with GluN1/GluN2A NMDA receptors isolated in membrane fractions of transiently transfected HEK cells. The resulting bound RNA−protein complexes were separated from unbound RNA using a nitrocellulose filter, and the RNA bound to GluN1/GluN2A receptors was eluted with 10 mM glutamate, collected, and used as a template for RT-PCR amplification for the next SELEX cycle. After three rounds of this positive selection, negative selection was interposed by incubating the RNA pool with GluA2 and GluK2 receptors expressed in HEK cells. RNA molecules which did not bind GluA2 and GluK2 were then collected and used for subsequent selection. Following three more positive selection rounds and two more negative selection rounds, the binding affinity of the ninth round RNA pool was evaluated. Radioligand binding experiments found the ninth round pool had a K_d of 210 ± 10 nM for GluN1/GluN2A receptors and no saturation binding for membranes containing GluA2 or GluK2 (Figure 1). The ninth round RNA pool was cloned and aligned using the ClustalX program. From sequences of the various cloned RNAs, a common consensus motif GCGGG was identified in 9 out of 24 clones (Table 1). The saturation binding curve of clone C26 from among those having the consensus sequence showed a K_d of 65 ± 3 nM (Figure 2B), considerably higher affinity than the K_d of 210 ± 10 nM observed for the pool. We hence used this clone for further analysis.

The secondary structure of the 90-nt RNA of clone C26 was predicted by Mfold and is shown in Figure 2A.[19] Based on this structure and the consensus motif GCGGG, observed in position 37−41, two truncated versions of the C26 aptamer, C26−50 and C26−31 (Figure 2A), were designed with lengths of 50-nt and 31-nt, respectively. Radioligand binding assays using membrane preparations of HEK 293T cells expressing GluN1/GluN2A receptors showed that both aptamers bound to NMDA receptors with the C26−50 aptamer having a K_d of 120 ± 15 nM while the C26-31 aptamer showed no saturation binding at concentrations up to 300 nM (Figure 2B).

To evaluate the functional effect of various aptamer we applied saturating concentrations of glutamate (10 mM) for 1 ms to outside-out patches expressing prototypical glutamate receptors either alone or in the continuous presence of 1 μM aptamer. This deactivation jump protocol has the advantage of closely mimicking the time course of synaptic activation in native tissue while retaining control over subunit composition.[20] Aptamer C26 robustly inhibited peak GluN1/GluN2A NMDA receptor responses (25 ± 2% peak responses, n = 7,

dx.doi.org/10.1021/cn500041k | ACS Chem. Neurosci. 2014, 5, 559−567

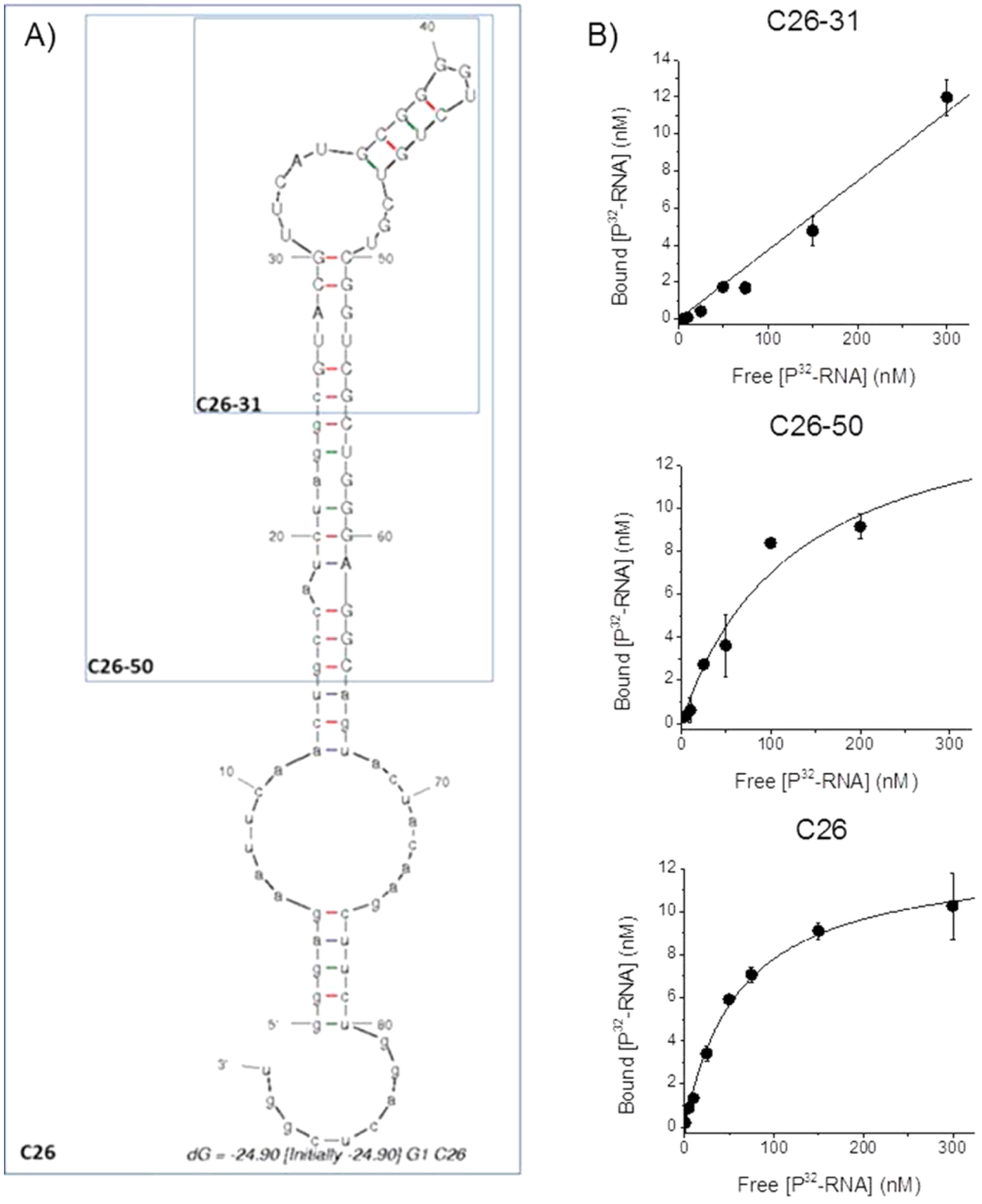

Figure 2. Truncation of candidate C26 aptamer. (A) Predicted secondary structure of the C26 aptamer showing segments truncated. (B) Radioligand binding curves for the indicated aptamer on GluN1/GluN2A NMDA receptors. Note the loss of saturating binding in C26−31 aptamer corresponding to a reduction in binding affinity.

Figure 3). Importantly, the same concentration of C26 showed negligible effects on peak currents from both GluA2 AMPA (83 ± 5% peak responses, n = 4) and kainate (KA) receptors (89 ± 2% peak responses, n = 4, Figure 3). We next examined the minimized constructs C26−50 and C26−31. The strong inhibition of C26 was preserved in the C26−50 construct which inhibited peak GluN2A responses 67% (33 ± 3% peak response, n = 6) while minimally perturbing AMPA (90.2 ± 0.3% peak response, n = 3) and KA receptor responses (96.6 ± 0.5% peak responses, n = 3, Figure 3). Consistent with the loss of saturation binding at low concentrations (Figure 2B), GluN2A peak inhibition was substantially reduced with C26−31 construct (67 ± 2% peak response, n = 6, Figure 3). Interestingly, selectivity was also lost, with C26−31 showing stronger inhibition at AMPA receptors (80 ± 3% peak response, n = 3) and especially KA receptors (73 ± 1% peak response, n = 3, Figure 3). We therefore selected C26−50 as our candidate aptamer for further functional characterization.

To determine the inhibitory potency of C26−50 at GluN2A containing NMDA receptors, we measured the peak current inhibition of long (2 s) 10 mM glutamate applications by the continual presence of varying concentrations of aptamer (Figure 4). As seen in Figure 4A, C26−50 produced a dose-dependent inhibition of peak responses in outside out patches. The IC_{50} for C26−50 calculated from these data on GluN2A peak responses was 1.3 ± 0.1 μM (n_h = 0.88 ± 0.04, n = 4−6 patches per point, Figure 4B). Interestingly, we observed that C26−50 also inhibited steady-state responses in these patches (Figure 4A), despite the presence of a super saturating concentration of glutamate (10 mM glutamate compared to an EC_{50} of 4 μM).[21] It was expected that C26−50 would be a competitive antagonist and as such high concentrations of

dx.doi.org/10.1021/cn500041k | ACS Chem. Neurosci. 2014, 5, 559−567

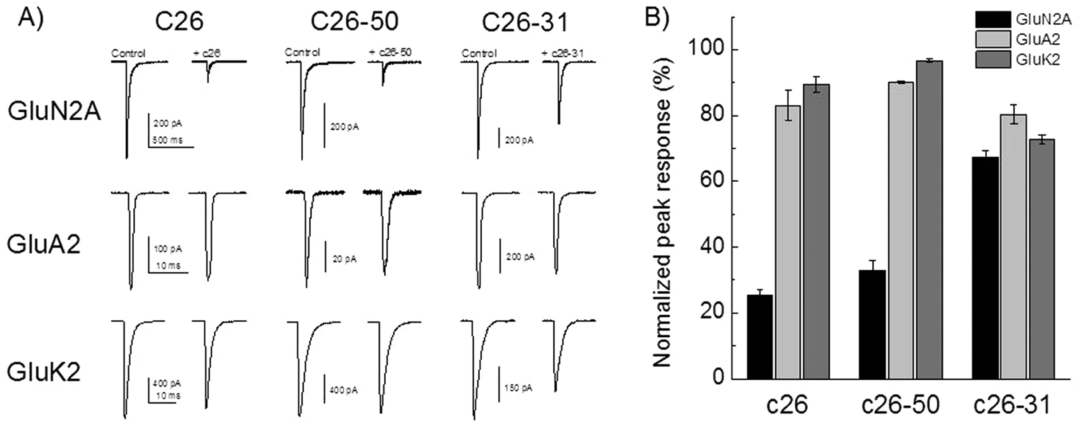

Figure 3. Glutamate receptor inhibition by truncated C26 aptamers. (A) Example responses to a 1 ms pulse of 10 mM glutamate in outside out patches containing GluN1/GluN2A NMDA receptors (upper row), GluA2 AMPA receptors (middle row), and GluK2 KA receptors (lower row) in the presence of 1 μM C26 (left column), C26−50 (middle column), and C26−31 (right column). Note NMDA receptor inhibition is reduced with C26−31. (B) Summary of inhibition by 1 μM of various truncated aptamers for each receptor type.

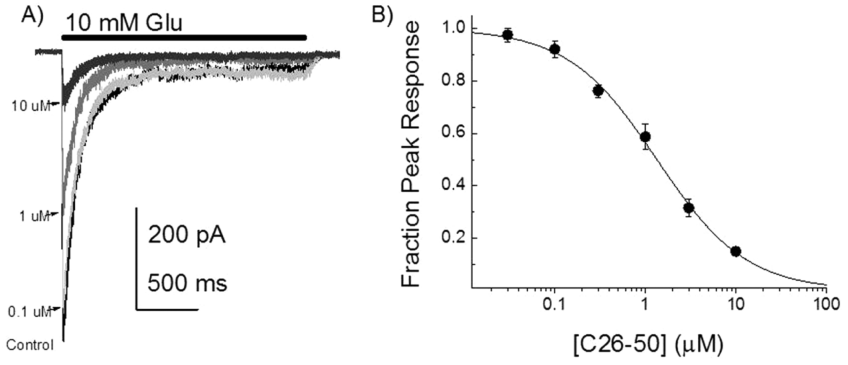

Figure 4. Inhibition curve of peak GluN1/GluN2A responses by the C26−50 aptamer. (A) Example responses of an outside-out patch containing GluN1/GluN2A receptors to a 2 s application of 10 mM glutamate alone or in the continual presence of the indicated concentration of C26−50 aptamer. (B) Summary of peak inhibition data.

glutamate would ultimately surmount inhibition of steady-state but not peak responses.[22,23] Instead, the persistent block by C26−50 at such high glutamate concentrations suggests that it acts as a noncompetitive antagonist. To further explore this, we carried out a competition experiment to determine if C26−50 acts as a competitive or noncompetitive antagonist. Under whole cell recording conditions with larger equilibrium response amplitudes, we attempted to surmount inhibition by C26−50 by increasing glutamate concentration. As seen in Figure 5, 1 μM C26−50 produces approximately 50% inhibition of the steady-state response when coapplied with 100 μM glutamate. Notably, this extent of inhibition is similar to that produced by 1 μM C26−50 for steady-state responses to 10 mM glutamate in patches, which is consistent with C26−50 being a noncompetitive antagonist (Figure 4). Increasing glutamate concentration to 1 mM in the same recording produced little to no relief of inhibition as would be predicted for a noncompetitive mechanism (Figure 5). Interestingly, a prominent tail current was observed at the end of agonist application (Figure 5A). This tail current likely reflects the C26−50 dissociating from the receptor while glutamate is still bound, allowing some activation to occur before glutamate finally dissociates. To further probe the mechanism of action of C26−50, we compared the glutamate dose−response curves in the absence of aptamer and the presence of 1 μM C26−50 which gives roughly 50% inhibition. In the absence of aptamer, steady-state responses to glutamate exhibited an EC_{50} of 5.4 ± 0.3 μM (n_h = 1.23 ± 0.07, n = 10 cells per point, Figure 5C) which is in excellent agreement with previous work.[20] The presence of 1 μM C26−50 induced small but statistically significant shift in the EC_{50} for glutamate with an EC_{50} of 9.6 ± 1.1 μM (n_h = 0.79 ± 0.07, n = 11, Figure 5C). We also constructed glutamate dose−response curves with 0.3 and 3 μM C26−50 which showed similar small but statistically significant right shifts in glutamate EC_{50}. Specifically, the EC_{50} for glutamate in the presence of 0.3 μM C26−50 was 8.0 ± 0.4 μM (n_h = 1.11 ± 0.06, n = 12) and was further shifted to 16 ± 2 μM (n_h = 0.76 ± 0.15, n = 12) with 3 μM C26−50. A Schild plot of these shifts in EC_{50} as a function of C26−50 concentration is shown in Figure 5D. The slope of this plot is 0.6 ± 0.1, clearly distinct from the slope of 1 expected for a pure competitive antagonist. Based on these results, we conclude that C26−50 is a noncompetitive antagonist of NMDA receptors with some allosteric effect on glutamate potency. Having established that C26−50 was selective noncompetitive inhibitor of NMDA receptor, we next moved on to assess C26−50's antagonistic potential in a more clinically relevant experiment.

To assess what, if any, therapeutic utility the C26−50 aptamer might have we examined the neuroprotective potential of these aptamers in an oxygen-glucose deprivation (OGD) model of neuronal cell death. Exposure of rat primary cortical

dx.doi.org/10.1021/cn500041k | ACS Chem. Neurosci. 2014, 5, 559−567

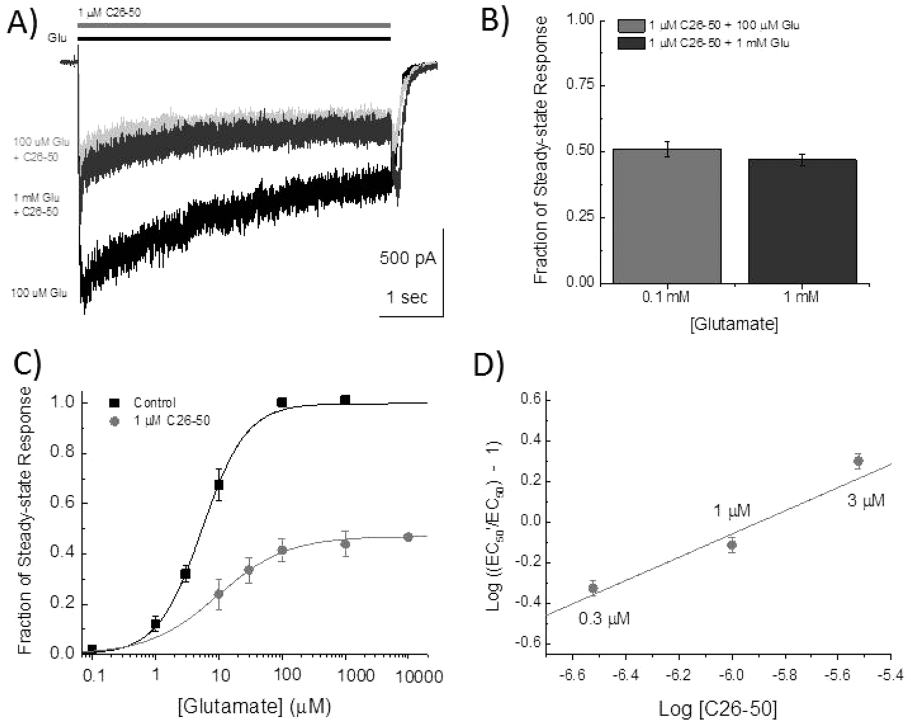

Figure 5. C26−50 is a noncompetitive inhibitor. (A) Representative whole cell responses to 100 mM glutamate alone (black trace), coapplied with 1 mM C26−50 (gray trace) or 1 mM glutamate coapplied with C26−50 (dark gray trace). Note that increasing glutamate concentration 10-fold does not relieve steady-state inhibition. (B) Summary of competition experiment showing additional glutamate did not relieve C26−50 inhibition. (C) Glutamate dose−response curves in the absence (black circles) and presence (red circles) of 1 μM C26−50. (D) Schild plot showing the shift in glutamate EC_{50} in the presence of various concentrations of C26−50 aptamer. The slope of the fit is 0.6 ± 0.1, confirming that C26−50 is a noncompetitive inhibitor.

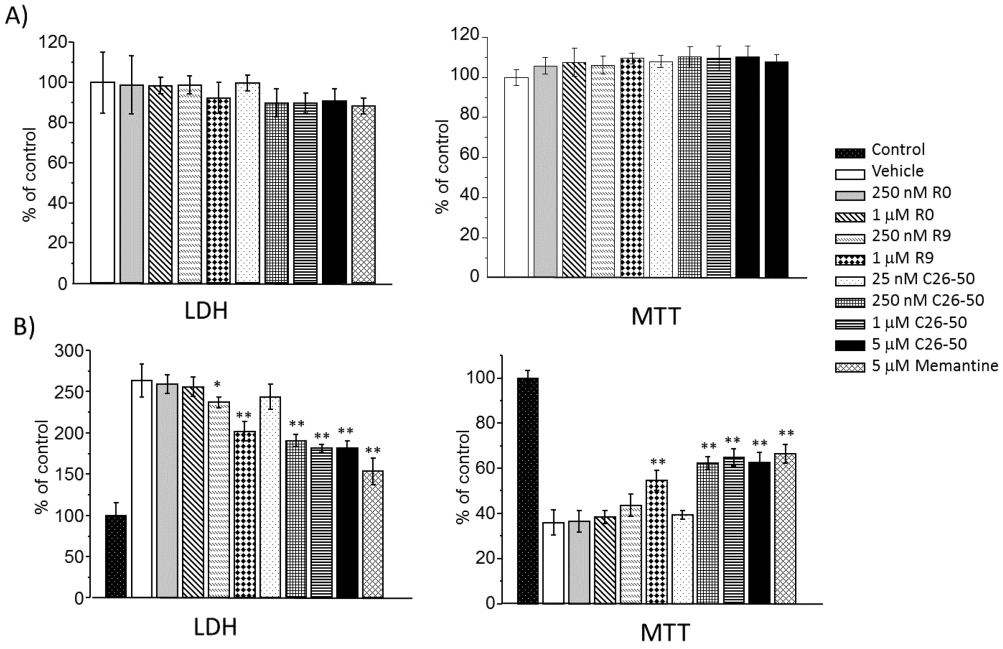

Figure 6. Neuronal injury and viability measured by LDH and MTT assays. (A) Percentages of neuronal survival in the presence of the indicated compounds without OGD. Note the absence of toxicity of these compounds. (B) Neuronal survival in the presence of the indicated compounds following OGD. Note that the C26−50 aptamer was neuroprotective at levels concentrations to memantine.

neurons to C26−50 aptamer or RNA pools (0th and ninth) at concentrations of up to 1 μM for 24 h did not produce cytotoxicity, as determined with LDH and MTT assays (Figure 6A). Rat primary cortical neurons incubated with RNA from pool 0 at concentrations up to 1 μM for 24 h during OGD showed no effect in both the LDH and MTT assay. However, cells incubated with 1 μM RNA from pool 9 showed statistically significant reductions in LDH release and increases in MTT

dx.doi.org/10.1021/cn500041k | ACS Chem. Neurosci. 2014, 5, 559−567

reactivity (Figure 6B), consistent with pool 9's higher affinity binding to GluN1/GluN2A receptors (Figure 1A). The C26−50 aptamer showed even stronger neuroprotection, with concentrations as low as 250 nM showing robust decreases in LDH release and increases in MTT reactivity (Figure 6B). Interestingly, no additional neuroprotection was observed at concentrations higher than 250 nM and this concentration also corresponded to the cell viability observed with the non-competitive NMDA receptors inhibitor memantine (Figure 6B). Taken together, these results demonstrate the selective isolation, characterization, and evaluation of C26−50, a novel RNA based antagonist of NMDA receptors with possible therapeutic applications.

Here we have used a modified SELEX procedure to develop a potent and selective RNA based antagonist of NMDA receptors. This alternating pattern of positive and negative selection produces an RNA pool with high affinity binding to the target subtype of the NMDA receptor and minimal detectable binding to the closely related AMPA and KA receptors (Figure 1). Subsequent cloning and screening isolated C26, an aptamer with high affinity for the NMDA receptor (Figure 2). Electrophysiological characterization, using brief 1 ms pulses of 10 mM glutamate to mimic synaptic transmission, revealed that this aptamer strongly inhibited NMDA receptors (Figure 3) with less of an effect on AMPA or KA receptors. Truncation experiments reduced the size of this aptamer to C26−50, a 50 base pair aptamer which retained potent NMDA receptor antagonism (IC_{50} = 1.3 ± 0.1 μM) and selectivity (Figures 3 and 4). Interestingly, both kinetic analysis and competition experiments suggest this aptamer acts via a noncompetitive mechanism (Figure 5). Crucially, low concentrations of C26−50 reduce OGD induced neuronal damage, as measured by LDH release and MTT reactivity (Figure 6B), just as well as the noncompetitive NMDA receptor antagonist memantine (Figure 6B).

There are several competitive and noncompetitive antagonists of the NMDA receptors that are currently available. However, the type of aptamer reported here offers several advantages over these traditional small molecule antagonists. First, the selectivity can be engineered. In the present case, we set out to deliberately evolve an antagonist to NMDA receptors with little to no inhibitory potency at AMPA or KA receptors. Such a goal is very time-consuming and expensive using classical methods of structure−activity studies and chemistry. Even in silico structure based design involves detailed structural information and computational resources. In contrast, our alternating negative and positive selection method was robust, efficient, and relatively inexpensive. Importantly, no prior structural information is required. Second, our aptamer can be easily truncated and optimized through simple cloning and in vitro translation instead of expensive and specialized chemical synthesis. Aptamers are also more amenable to chemical alternations and can be packaged together with modern drug delivery methods such as immunoliposomes.[10−12] This combination of deliberately evolved selectivity and tissue-specific, and perhaps even brain region specific, delivery may open up new avenues of glutamatergic interventions in various disease states.

Previous RNA aptamers developed to inhibit ionotropic glutamate receptors have all focused on inhibiting the AMPA class of these receptors.[14,24−26] These studies have isolated RNA sequences capable of blocking the AMPA receptor with high affinity[24,26] and also show some degree of state-dependent inhibition[14] as well as therapeutic potential.[27] However, from a drug developmental perspective, AMPA receptors are difficult targets as their signaling is so prevalent in the CNS and the subunits are highly related, making subtype selectivity a persistent problem. Moreover, AMPA receptors are often accompanied by several auxiliary proteins which can regulate their function and alter drug responses.[28] In contrast, NMDA receptors make more attractive targets as there are fewer auxiliary proteins which alter pharmacology, more room for subtype specificity, and less frequent signaling. This advantage is further evidenced by the number of NMDA antagonists that have been involved in clinical trials compared to AMPA receptor antagonists.[1] Here we report the first description of an aptamer evolved specifically for GluN1/GluN2A NMDA receptors. We evolved this aptamer with a combination of positive selection to extract sequences with high affinity and negative selection to suppress sequences which show poor selectivity. Our result was the C26−50 aptamer which binds with nanomolar affinity to the GluN1/GluN2A NMDA receptor (K_d = 120 ± 15 nM, Figure 2) and inhibits activation of NMDA receptors by high concentrations of glutamate with an IC_{50} of 1.3 ± 0.1 μM (Figure 3). Most importantly, this aptamer shows neuroprotective effects at levels comparable to memantine, the only NMDA antagonist to be approved for clinical use to date.[1] Combining this candidate aptamer with specific delivery methods may open up new avenues of therapeutic intervention.

METHODS

Chemicals. Glutamate was purchased from Sigma (St. Louis, MO), [α-^{32}P]-ATP (25 Ci/mmol), and L-[α-^{3}H]-glutamic acid (49.0 Ci/mmol) were from MP Bio (Solon, OH) and PerkinElmer (Boston, MA). 2′-Fluoro-2′-deoxyuridine-5′-triphosphate (2′-F-dUTP) and 2′-fluoro-2′-deoxycytidine-5′-triphosphate (2′-F-dCTP) were purchased from Trilink Technologies (San Diego, CA), and ATP and GTP were from Ambion (Austin, TX). Memantine was obtained from Tocris (Bristol, U.K.).

Cell Culture and Protein Expression. HEK 293T cells (ATCC, CRL-11268) were maintained in DMEM supplemented with 10% FBS and 5% Pen/Strep at 37 °C and 5% CO_2. Cells were transfected using Lipofectamine 2000 following manufacturer's instructions (Invitrogen, Carlsbad, CA). The cDNAs for GluN1 and GluN2A were obtained from Dr. Nakanishi (Kyoto University, Japan), GluA2-flip was obtained from Dr. Peter Seeburg (Max Planck Institute, Germany), and GluK2 was provided by Dr. Kathyrn Partin (Colorado State University, Fort Collins, CO). For SELEX and radioactive ligand binding experiments, transfected cells were harvested 48 h after transfection as described previously.[29] For membrane enrichment, cells were resuspended in 20 mM HEPES buffer (pH 7.4) containing 250 mM sucrose, 1 mM EDTA, and EDTA-free Complete Protease Inhibitor Mixture (Roche Diagnostics). Then 0.1 M NaCl and 0.4 mM $MgSO_4$ were added to the buffer, and cells were centrifuged for 1 h at 100 000g and 4 °C. The pellet was resuspended in 20 mM HEPES (pH 7.4) and 1 mM EDTA buffer and ultracentrifuged again and then resuspended in SELEX buffer, which contained 145 mM NaCl, 5.3 mM KCl, 1.8 mM $CaCl_2$, 1.7 mM MgCl, and 25 mM HEPES (pH 7.4) for expression verifying using western analysis.

Preparation of 2′-F-Pyrimidine RNA Pool. The PAGE-purified 108-nt single-stranded (ss) DNA library and two HPLC-purified primers were obtained from Sigma-Genosys (The Woodlands, TX). The synthetic ssDNA template contained a 40-nt central randomized region flanked by two constant regions (5′-ACC GAG TCC AGA AGC TTG TAG TAC T-N40-GCC TAG ATG GCA GTT GAA TTC TCC CTA TAG TGA GTC GTA TTA C-3′). The two primers used for the generation of double-stranded (ds) DNA template pool were: 5′-GTA ATA CGA CTC ACT ATA GGG AGA ATT CAA CTG

dx.doi.org/10.1021/cn500041k | ACS Chem. Neurosci. 2014, 5, 559−567

CCA TCT A-3′ (P-40), and 5′-ACC GAG TCC AGA AGC TTG TAG T-3′ (P-22). For generating the 10^{15} library, error-prone PCR amplification was performed.[30,31] The initial nuclease resistant 2′-F-pyrimidine RNA pool (RNA Pool 0) was obtained by in vitro transcription of the 108-nt dsDNA template pool using T7 RNA polymerase (Ambion, Austin, TX), ATP, GTP, and 2′-fluoro-modified pyrimidine nucleotide triphosphates.[32] The template DNA was removed using RNase-free DNase I (2 U/μL) (Ambion). The RNA thus obtained was heat denatured at 65 °C and renatured at room temperature to allow the formation of secondary structures, and its integrity verified using an 8% denaturing polyacrylamide gel.

Displacement SELEX. GluN1/GluN2A membranous protein was used as a target for the SELEX experiments. The molar ratio of the RNA pool to protein started from 1:1 and was gradually increased to a final ratio of 100:1 in round 9. In each round, RNA pool−protein complex was incubated in SELEX buffer supplemented with 0.3 μg/μL yeast t-RNA (pH 7.4), for 40 min. Bound and unbound RNAs were filter separated using a nitrocellulose membrane (Millipore, Billerica, MA).[31,33] After washing with SELEX buffer, the bound RNA was displaced with 10 mM glutamate. The collected supernatant containing the displaced RNA was phenol- and chloroform-extracted, and the purified RNA was used as a template for reverse-transcription (RT) PCR amplification to obtain the DNA pool for the initiating next SELEX round. For counter SELEX or negative selection, GluA2 and GluK2 membranous protein was used, and unbound RNA passing through the membrane was collected during successive rounds. Following 9 cycles of in vitro selection, the RNA pool was cloned into the pGEM3Z vector (Promega, Madison, WI) for subsequent DNA sequencing and aptamer characterization.

Radioligand Binding. The binding affinities of the RNA aptamer pools and individual clones were determined by saturation binding analysis using HEK 293 cell membranes transiently expressing GluN1/GluN2A, GluA2, or GluK2. Constant amounts of membrane protein (10 μg) were incubated with increasing concentrations of the [^{32}P]-labeled individual RNA aptamer (1−300 nM) in SELEX buffer for 1h at room temperature and passed through nitrocellulose membranes using a vacuum manifold (Millipore). Bound radioligand−protein complex was washed three times and radioactivity determined using a liquid scintillation counter. Nonspecific binding of [^{32}P]-RNA was determined by including 10 mM glutamate in the binding assay. The K_d values for the ligands were determined using eq 1:

$$y = \frac{(xB_{max})}{(x + K_d)} \quad (1)$$

where y is the concentration of bound radioactive ligand given x concentration of free ligand, B_{max} is the maximum amount of bound radioactive ligand, and K_d is the dissociation constant.

Electrophysiology. Outside-out patch recordings were performed on HEK 293T cells transfected with either GluN1 and GluN2A (1:3 μg cDNA/10 mL media), GluA2 (5 μg cDNA), or GluK2 (2 μg cDNA) and eGFP as a marker (1 μg cDNA) using Lipofectamine 2000 at a 1:1.5 ratio of cDNA to lipofectamine. Following 24 to 48 h of transfection, outside-out patches were pulled from eGFP expressing cells using thick walled borosilicate glass pipettes of 3−5 MΩ, coated with beeswax, fire-polished, and filled with a solution which contained (in mM) 135 CsF, 33 CsOH, 11 EGTA, 10 HEPES, 2 $MgCl_2$, 1 $CaCl_2$, pH 7.4. External solutions were made in DEPC treated water and composed of (in mM) 150 NaCl, 10 HEPES, 1 $CaCl_2$, and 0.1 glycine and adjusted to pH 7.4 with 5 N NaOH. All recordings were performed with a holding potential of −60 mV using an Axopatch 200B amplifier (Molecular Devices, Sunnyvale, CA) acquired at 40 kHz and filtered at 10 kHz (8-pole Bessel) under the control of pCLAMP 10 software. Series resistances (3−10 MΩ) were routinely compensated by >95% where the amplitude exceeded 100 pA. Rapid application was performed using home-built theta (Warner Instruments, Hamden, CT) or multibarrel (Vitrocom, Mountain Lake, NJ) glass application pipettes, pulled to 100−150 μm, and translated using a piezoelectric microstage (Burleigh Instruments). Solution exchange as estimated from open tip potentials was 100−300 μs (10−90% rise-time). For whole cell experiments, a custom built multibarrel perfusion system was driven by solenoid valves (Warner Instruments). Inhibition curves were fit with eq 2:

$$y = \frac{I_{max}}{\left(1 + \left(\frac{x}{IC_{50}}\right)^{n_h}\right)} \quad (2)$$

where y is the peak current at aptamer concentration x, I_{max} is the maximal peak current in the absence of aptamer, IC_{50} is the concentration of aptamer producing half-maximal inhibition, and n_h is the Hill coefficient. Dose−response curves were fit with eq 3:

$$y = \frac{I_{max}}{\left(1 + \left(\frac{EC_{50}}{x}\right)^{n_h}\right)} \quad (3)$$

where y is the peak current at aptamer concentration x, I_{max} is the maximal peak current in the absence of aptamer, EC_{50} is the concentration of glutamate producing half-maximal response, and n_h is the Hill coefficient. Statistical significance was evaluated using the two-tailed Student's t test.

Primary Cortical Neuron Cultures. Primary neuron cultures were prepared from E15 to E16 day rat embryos as described by Zhao and co-workers.[34] Neocortices were dissected and dissociated by trituration. The dissociated cells were then plated onto poly-L-lysine coated culture plates in Neurobasal Medium with B27 at a density of 700/mm^2 and cultured in a 5% CO_2 and 21% O_2 incubator at 37.0 ± 0.5 °C. The culture medium was changed every 3 days. After a total of 10 days in culture, the cells were used for experiments.

Oxygen-Glucose-Deprivation Injury. The cell injury was induced by subjecting the cultured cells to oxygen-glucose-deprivation (OGD) for 1 h as previously described.[35] In a gastight humidified chamber, 5% CO_2/95% N_2 gas mixture was flushed for 10 min and then cells were cultured at 37.0 ± 0.5 °C for 1 h. For OGD, the media was changed to a glucose-free mixture (Invitrogen, Carlsbad, CA), and oxygen was removed for 1 h at 37 °C. At the end of OGD injury, glucose was added into the cultures, and the culture plates were returned to the original culture incubator for reoxygenation. The cell survival/death was measured 24 h after OGD. For testing RNA aptamers, 0.025, 0.25, 1, and 5 μM of the C26−50 aptamer or the 0.25 and 1 μM of zeroth (initial RNA pool) and ninth round RNA pools were added directly to the culture medium 15 min before OGD. The RNA aptamer remained in the media throughout the experiment. The initial RNA pool 0 was used as negative control while the NMDA receptor antagonist memantine (5 μM) was included as positive control.

LDH Assay and MTT Assay. Assessment of neuronal injury was performed by measuring the release of lactate dehydrogenase (LDH) into the culture media using an LDH assay kit (Promega, Madison, WI). A volume of 50 μL of culture media was collected from each culture well and incubated with 50 μL of the LDH assay reagent for 30 min in a 96-well plate. The colorimetric value (OD) was determined using an ELISA Reader (Bio-Rad) at 490 nm. The data were expressed as percentage over control. The neuronal viability after OGD was measured using a 3-(4,5-dimethylthiazol-2-yl)-2,5-diphenyltetrazolium bromide (MTT) kit (Promega, Madison, WI). The soluble tetrazolium was added into the neuron culture media at 20 h after the onset of OGD and incubated for 4 h. The insoluble formazan that formed in the metabolically viable neurons was dissolved with a mixture of isopropanol/formic acids (95/5), and the optical densities were measured at 545 nm.

Statistical Analysis. All data were expressed as mean ± SEM. Two independent OGD experiments were performed with each condition having five duplicates (5 culture wells each time). The data were analyzed using Prism and InStat (GraphPad Software Inc., San Diego, CA). One-way analysis of variance (ANOVA) followed by the Newman-Keuls post-test was used to evaluate the difference among the groups. $P \leq 0.05$ (represented by *) and $P \leq 0.001$ (represented by **) were considered significant.

AUTHOR INFORMATION

Corresponding Author

*Mailing address: MSB 6.174, 6431 Fannin, Department of Biochemistry and Molecular Biology, University of Texas Health Science Center, Houston, Texas 77030, USA. E-mail: vasanthi.jayaraman@uth.tmc.edu.

Author Contributions

‖G.L. and D.M.M. contributed equally to the manuscript. G.L. performed aptamer development and radioligand binding studies. D.M.M. carried out electrophysiology experiments. X.Z. performed the OGD assay and analysis. H.U., J.A., and V.J. designed the study. G.L., D.M.M., and V.J. drafted the manuscript which was approved by all authors.

Funding

This work was supported by a Muscular Dystrophy Association Grant MDA199041 (V.J.) and in part by National Institutes of Health Grant GM094246 (V.J.), and an American Heart Association postdoctoral fellowship (D.M.M). H.U. acknowledges grant support by Fundação de Amparo à Pesquisa do Estado de São Paulo (FAPESP), Conselho Nacional de Desenvolvimento Cient ífico e Tecnol ógico (CNPq), and the Provost's Office for Research of the University of São Paulo, Grant Number: 2011.1.9333.1.3 (NAPNAUSP), Brazil.

Notes

The authors declare no competing financial interest.

ACKNOWLEDGMENTS

We wish to thank members of the Jayaraman lab for critical reading of the manuscript.

REFERENCES

(1) Traynelis, S. F., Wollmuth, L. P., McBain, C. J., Menniti, F. S., Vance, K. M., Ogden, K. K., Hansen, K. B., Yuan, H., Myers, S. J., and Dingledine, R. (2010) Glutamate receptor ion channels: structure, regulation, and function. *Pharmacol. Rev. 62*, 405−496.

(2) Kalia, L. V., Kalia, S. K., and Salter, M. W. (2008) NMDA receptors in clinical neurology: excitatory times ahead. *Lancet Neurol. 7*, 742−755.

(3) Calabresi, P., Centonze, D., Cupini, L. M., Costa, C., Pisani, F., and Bernardi, G. (2003) Ionotropic glutamate receptors: still a target for neuroprotection in brain ischemia? Insights from in vitro studies. *Neurobiol. Dis. 12*, 82−88.

(4) Caplan, L. R. (1998) Stroke treatment: promising but still struggling. *JAMA, J. Am. Med. Assoc. 279*, 1304−1306.

(5) Martinez-Vila, E., and Sieira, P. I. (2001) Current status and perspectives of neuroprotection in ischemic stroke treatment. *Cerebrovasc. Dis. 11* (Suppl 1), 60−70.

(6) Plum, F. (2001) Neuroprotection in acute ischemic stroke. *JAMA, J. Am. Med. Assoc. 285*, 1760−1761.

(7) Winblad, B., Jones, R. W., Wirth, Y., Stoffler, A., and Mobius, H. J. (2007) Memantine in moderate to severe Alzheimer's disease: a meta-analysis of randomised clinical trials. *Dementia Geriatr. Cognit. Disord. 24*, 20−27.

(8) Aarsland, D., Ballard, C., Walker, Z., Bostrom, F., Alves, G., Kossakowski, K., Leroi, I., Pozo-Rodriguez, F., Minthon, L., and Londos, E. (2009) Memantine in patients with Parkinson's disease dementia or dementia with Lewy bodies: a double-blind, placebo-controlled, multicentre trial. *Lancet Neurol. 8*, 613−618.

(9) De Keyser, J., Van de Velde, V., Schellens, R. L., Hantson, L., Tritsmans, L., Gheuens, J., Van Peer, A., Woestenborghs, R., Franke, C. L., and van Gorp, J. (1997) Safety and pharmacokinetics of the neuroprotective drug lubeluzole in patients with ischemic stroke. *Clin. Ther. 19*, 1340−1351.

(10) Dua, P., Kim, S., and Lee, D. K. (2011) Nucleic acid aptamers targeting cell-surface proteins. *Methods (San Diego, CA, U.S.) 54*, 215−225.

(11) Ruigrok, V. J., Levisson, M., Eppink, M. H., Smidt, H., and van der Oost, J. (2011) Alternative affinity tools: more attractive than antibodies? *Biochem. J. 436*, 1−13.

(12) Tan, W., Wang, H., Chen, Y., Zhang, X., Zhu, H., Yang, C., Yang, R., and Liu, C. (2011) Molecular aptamers for drug delivery. *Trends Biotechnol. 29*, 634−640.

(13) Smuc, T., Ahn, I. Y., and Ulrich, H. (2013) Nucleic acid aptamers as high affinity ligands in biotechnology and biosensorics. *J. Pharm. Biomed. Anal. 81−82*, 210−217.

(14) Huang, Z., Han, Y., Wang, C., and Niu, L. (2010) Potent and selective inhibition of the open-channel conformation of AMPA receptors by an RNA aptamer. *Biochemistry 49*, 5790−5798.

(15) Hess, G. P., Ulrich, H., Breitinger, H. G., Niu, L., Gameiro, A. M., Grewer, C., Srivastava, S., Ippolito, J. E., Lee, S. M., Jayaraman, V., and Coombs, S. E. (2000) Mechanism-based discovery of ligands that counteract inhibition of the nicotinic acetylcholine receptor by cocaine and MK-801. *Proc. Natl. Acad. Sci. U.S.A. 97*, 13895−13900.

(16) Blank, M., Weinschenk, T., Priemer, M., and Schluesener, H. (2001) Systematic evolution of a DNA aptamer binding to rat brain tumor microvessels. selective targeting of endothelial regulatory protein pigpen. *J. Biol. Chem. 276*, 16464−16468.

(17) Cheng, C., Chen, Y. H., Lennox, K. A., Behlke, M. A., and Davidson, B. L. (2013) In vivo SELEX for Identification of Brain-penetrating Aptamers. *Mol. Ther. 2*, e67.

(18) Ulrich, H., Martins, A. H., and Pesquero, J. B. (2004) RNA and DNA aptamers in cytomics analysis. *Cytometry, Part A 59*, 220−231.

(19) Zuker, M. (2003) Mfold web server for nucleic acid folding and hybridization prediction. *Nucleic Acids Res. 31*, 3406−3415.

(20) Clements, J. D., Lester, R. A., Tong, G., Jahr, C. E., and Westbrook, G. L. (1992) The time course of glutamate in the synaptic cleft. *Science 258*, 1498−1501.

(21) Paoletti, P., Bellone, C., and Zhou, Q. (2013) NMDA receptor subunit diversity: impact on receptor properties, synaptic plasticity and disease. *Nat. Rev. Neurosci. 14*, 383−400.

(22) Maclean, D. M., and Bowie, D. (2011) Transmembrane AMPA receptor regulatory protein regulation of competitive antagonism: a problem of interpretation. *J. Physiol. 589*, 5383−5390.

(23) Wyllie, D. J., and Chen, P. E. (2007) Taking the time to study competitive antagonism. *Br. J. Pharmacol. 150*, 541−551.

(24) Du, M., Reid, S. A., and Jayaraman, V. (2005) Conformational changes in the ligand-binding domain of a functional ionotropic glutamate receptor. *J. Biol. Chem. 280*, 8633−8636.

(25) Huang, Z., Pei, W., Jayaseelan, S., Shi, H., and Niu, L. (2007) RNA aptamers selected against the GluR2 glutamate receptor channel. *Biochemistry 46*, 12648−12655.

(26) Park, J. S., Wang, C., Han, Y., Huang, Z., and Niu, L. (2011) Potent and selective inhibition of a single alpha-amino-3-hydroxy-5-methyl-4-isoxazolepropionic acid (AMPA) receptor subunit by an RNA aptamer. *J. Biol. Chem. 286*, 15608−15617.

(27) Du, M., Ulrich, H., Zhao, X., Aronowski, J., and Jayaraman, V. (2007) Water soluble RNA based antagonist of AMPA receptors. *Neuropharmacology 53*, 242−251.

(28) Yan, D., and Tomita, S. (2012) Defined criteria for auxiliary subunits of glutamate receptors. *J. Physiol. 590*, 21−31.

(29) Sirrieh, R. E., MacLean, D. M., and Jayaraman, V. (2013) Amino-terminal domain tetramer organization and structural effects of zinc binding in the *N*-methyl-D-aspartate (NMDA) receptor. *J. Biol. Chem. 288*, 22555−22564.

(30) Ulrich, H., Martins, A. H., and Pesquero, J. B. (2005) RNA and DNA aptamers in Cytomics Analysis. In *Current Protocols in Cytometry* (Robinson, J. R., Darzynkiewic, Z., Hyu,W., Orfa, A., Rabinovitch, P., Eds.), unit 7.28, pp 1−39, Wiley, New York.

(31) Ulrich, H., Ippolito, J. E., Pagan, O. R., Eterovic, V. A., Hann, R. M., Shi, H., Lis, J. T., Eldefrawi, M. E., and Hess, G. P. (1998) In vitro selection of RNA molecules that displace cocaine from the membrane-

bound nicotinic acetylcholine receptor. *Proc. Natl. Acad. Sci. U.S.A. 95*, 14051−14056.
(32) Ulrich, H., Magdesian, M. H., Alves, M. J., and Colli, W. (2002) In vitro selection of RNA aptamers that bind to cell adhesion receptors of Trypanosoma cruzi and inhibit cell invasion. *J. Biol. Chem. 277*, 20756−20762.
(33) Ulrich, H., and Wrenger, C. (2013) Identification of aptamers as specific binders and modulators of cell-surface receptor activity. *Methods Mol. Biol. 986*, 17−39.
(34) Zhao, X., Ou, Z., Grotta, J. C., Waxham, N., and Aronowski, J. (2006) Peroxisome-proliferator-activated receptor-gamma (PPARgamma) activation protects neurons from NMDA excitotoxicity. *Brain Res. 1073−1074*, 460−469.
(35) Kim, D. H., Zhao, X., Tu, C. H., Casaccia-Bonnefil, P., and Chao, M. V. (2004) Prevention of apoptotic but not necrotic cell death following neuronal injury by neurotrophins signaling through the tyrosine kinase receptor. *J. Neurosurg. 100*, 79−87.